Journal of Catalysis 269 (2010) 309–317

Contents lists available at ScienceDirect

Journal of Catalysis

journal homepage: www.elsevier.com/locate/jcat

Methanol oxidation over model cobalt catalysts: Influence of the cobalt oxidation state on the reactivity

S. Zafeiratos [a,*], T. Dintzer [a], D. Teschner [b], R. Blume [b], M. Hävecker [b], A. Knop-Gericke [b], R. Schlögl [b]

[a] LMSPC, UMR 7515 du CNRS, 25 Rue Becquerel, 67087 Strasbourg, France
[b] Fritz-Haber-Institut der Max-Planck-Gesellschaft, Faradayweg 4-6, 14195 Berlin, Germany

ARTICLE INFO

Article history:
Received 20 July 2009
Revised 1 October 2009
Accepted 12 November 2009

Keywords:
Cobalt catalyst
Cobalt oxides
Methanol oxidation
In situ XPS
In situ XAS
Reaction intermediates
Fischer–Tropsch synthesis

ABSTRACT

X-ray photoelectron and absorption spectroscopies (XPS and XAS) combined with *on-line* mass spectrometry were applied under working catalytic conditions to investigate methanol oxidation on cobalt. Two cobalt oxidation states (Co_3O_4 and CoO) were prepared and investigated as regards their influence on the catalytic activity and selectivity. In addition adsorbed species were monitored in the transition of the catalyst from a non-active state, to an active one. It is shown that the surface oxidation state of cobalt is readily adapted to the oxygen chemical potential in the CH_3OH/O_2 reaction mixture. In particular, even in oxygen-rich mixtures the Co_3O_4 surface is partially reduced, with the extent of surface reduction following the methanol concentration. The reaction selectivity depends on the cobalt oxidation state, with the more reduced samples favouring the partial oxidation of methanol to formaldehyde. In the absence of oxygen, methanol effectively reduces cobalt to the metallic state, also promoting H_2 and CO production. Direct evidence of methoxy and formate species adsorbed on the surface upon reaction was found by analysing the O 1s and C 1s photoelectron spectra. However, the surface coverage of those species was not proportional to the catalytic activity, indicating that they might also act as reaction inhibitors.

1. Introduction

Our current understanding of heterogeneous catalysis is to a large extent built on post-reaction (*ex situ*) analysis of the catalysts and deductions based on kinetic experiments. A key problem was the lack of surface-sensitive techniques that could provide spectroscopic information at pressures relevant to the catalysis process. The situation in catalyst characterization is gradually changing, and today a variety of techniques are available that may provide detailed atomic-scale structural and chemical insight into complex heterogeneous catalysts exposed to controlled environments that closely match the working conditions [1–3]. These studies showed that the structure of a heterogeneous catalyst is dynamic and is intimately dependent on the reaction conditions. Such dynamic changes have, for example, been observed on a Cu and Ru catalyst during methanol oxidation, indicating that the active state of the catalyst exists only during the process of catalysis [4–7].

Cobalt and its oxides (CoO and Co_3O_4) exhibit interesting electronic and magnetic properties and are used as catalysts in a range of reactions. Perhaps the major application of cobalt-based catalysts is in the Fischer–Tropsch synthesis, since cobalt has been shown to efficiently convert syn gas ($CO + H_2$) to methane or liquid fuels [8–11]. Other applications of cobalt catalysts include partial oxidation reactions [12] and decomposition of methane to form hydrogen and carbon nanotubes or filamentous carbon [13,14]. Recently cobalt has been proposed as a very promising catalyst to replace noble metals for H_2 production by steam reforming of ethanol [15,16]. Pure cobalt oxide surface phases have seldom been investigated with respect to their catalytic properties [17–19] and always by *ex situ* methods. While this has provided valuable information, the question of whether or not the active surface state "survives" after reaction remains unanswered.

In the present work, ambient pressure photoelectron and soft X-ray absorption spectroscopies were applied under working catalytic conditions, to investigate methanol oxidation on cobalt. Previous studies of methanol adsorption on Co(0 0 0 1) surface indicated dissociative adsorption and decomposition of methanol to CO and H_2 upon annealing [20]. On the other hand, on cobalt oxide surfaces methanol is molecularly chemisorbed at room temperature, while dissociation and formation of formate and formaldehyde species was observed upon annealing [19]. In the presence of oxygen both, partial (carbon monoxide, formaldehyde ext) and complete, oxidation products (carbon dioxide) can be produced depending on the conditions. A detail description of the most prominent reaction paths has been given elsewhere [5–7]. Our previous in situ photoelectron spectroscopy studies of methanol oxidation on Ru and Cu suggested that the active catalyst state is

* Corresponding author.
E-mail address: spirosz@ecpm.u-strasbg.fr (S. Zafeiratos).

0021-9517/$ - see front matter © 2009 Elsevier Inc. All rights reserved.
doi:10.1016/j.jcat.2009.11.013

neither the metal nor the stoichiometric oxides, but rather a "transient oxidized state" controlled by the chemical potential of gas phase oxygen [2 and reference therein].

Acquiring fundamental understanding of the reaction networks of methanol on cobalt is important for further development of processes such as production of formaldehyde and for operation of direct methanol fuel cells. On the other hand, methanol may also serve as a simple model compound for the study of the oxidation of the other, more complex alcohols, like ethanol and glycerol [21]. The aim of this work is to discover if cobalt undergoes dynamic variations under reaction conditions and to understand the role of different cobalt oxidation states in the reaction pathways.

2. Materials and methods

In situ X-ray photoelectron and absorption spectroscopies (XPS and XAS, respectively) were performed at ISISS beamline at BESSY in Berlin, in a setup described elsewhere [2,4]. The soft X-ray absorption spectra of the Co $L_{3,2}$ edges were recorded in the Total Electron Yield (TEY) mode, enhanced by additional electrons created by ionization of the gas phase above the sample. The 0.5 mm thick and 5 mm diameter Co(0 0 0 1) single crystal was placed on a sample holder, which could be heated from the rear by an IR laser (cw, 808 nm). The temperature was measured by a K-type thermocouple fixed onto the sample surface. The Co crystal was pre-treated in the XPS reaction cell by oxidation (0.2 mbar O_2 at 520 K) and reduction (0.2 mbar H_2 at 520 K) cycles, until all residual surface carbon disappeared. The same procedure was repeated after each reaction cycle to "refresh" the surface. The reaction mixture was introduced after cooling down the sample at 300 K with an overall pressure of 0.1–0.3 mbar. Consequently the sample was heated to 520 K (by 5 K/min) where photoemission and absorption spectra were recorded. Preparation of Co_3O_4 and metallic Co surfaces was attained after 30 min annealing in 0.2 mbar O_2 and H_2 respectively, at 520 K. The CoO surface was formed by heating metallic Co at 450 K in 0.2 mbar H_2 and consequently introducing traces of O_2 (~5–10% of the hydrogen pressure). Few minutes under these conditions were adequate to form a thick CoO layer on the Co crystal, as judged by XPS.

CH_3OH, O_2 and H_2 gas flow into the reaction cell was controlled using calibrated mass flow controllers. A differentially pumped quadrupole mass spectrometer (QMS) was connected through a leak valve to the experimental cell and the gas phase composition was simultaneously monitored by *on-line* mass spectrometry to the spectroscopic characterization of the surface. The decrease of CH_3OH ($m/e = 31$) QMS intensity was used to calculate CH_3OH conversion under reaction conditions. Relative product selectivities were calculated by the increase of the H_2 ($m/e = 2$), CO ($m/e = 28$), CH_2O ($m/e = 30$) and CO_2 ($m/e = 44$) QMS intensities induced by the catalytic reaction. A correction of the ion current signals of $m/e = 28$ and 30 due to CH_3OH fragment (20% and 25% of $m/e = 31$, respectively) was also taken into account. It should be noted that, since QMS signals are not calibrated to the sensitivity factor of each gas, only the comparison of selectivities between various conditions (*relative selectivity*), and not absolute values are considered here. For the sake of simplicity we refer only to selectivity in the following.

Photoemission spectra were recorded both during temperature rising and stationery conditions. The typical duration of an experiment was about 90 min, while the acquisition time of each spectrum was between 1 and 2 min. Therefore, the same energy region (e.g. Co $2p_{3/2}$) was recorded in different stages of the stationery experiments. As a consequence, whenever combined catalytic and spectroscopic data are presented they refer to the same experimental stage. Two methanol-to-oxygen mixing ratios (MR) 1:5 and 2:1 were studied and are referred to here as MR = 0.2 and 2, respectively. The Co 2p, O 1s and C 1s spectra were recorded using appropriately selected photon energies, resulting in photoelectrons with two characteristic kinetic energies for each spectrum, namely 180 and 580 eV ($\lambda_{[180eV]}/\lambda_{[580eV]} = 0.56$, where λ is the photoelectron attenuation length) [22]. In that way, information of two different depths was collected providing a non destructive depth analysis. For the calculations all spectra were normalized by the storage ring current and the energy-dependent incident photon flux, which was measured prior to the measurements using a gold foil with known quantum efficiency. The photon flux obtained has been corrected for higher diffraction orders that contribute only to the background but not to the peak intensity in XPS. The spectra presented here are rescaled to facilitate the observation of peak characteristics. The binding energy (BE) scale was calibrated with respect to the Fermi level of the electron analyzer. The oxidized surface showed no electrostatic charging. Curve fitting of the O 1s and C 1s peaks was performed based on a mixed Gaussian/Lorentzian function. XPS and XAS peaks of Co were fitted using line shapes recorded on reference samples. Background subtraction was carried out by using the Shirley method. Quantitative calculations were performed using normalized Co 2p, O 1s, C 1s intensities, taking into account the photon-energy dependence of the atomic subshell photoionization cross sections [23].

3. Results

3.1. The dynamic transformation of cobalt upon changes in the reaction mixture

There are two stable bulk phases of cobalt oxide, i.e., the fcc-type rocksalt structure of CoO and the cubic spinel structure of Co_3O_4. The thermodynamically stable form of cobalt oxide under ambient temperature and pressure conditions is the Co_3O_4 spinel phase [9,24]. Therefore, initially we investigated how pre-oxidized cobalt surfaces respond to different reactant-mixing ratios (MRs). Two MRs (0.2 and 2), as well as pure methanol, were studied at separate reaction cycles. Fig. 1 displays photoemission and absorption spectra of Co 2p core level ($L_{3,2}$ edge in absorption spectroscopy nomenclature) obtained from a cobalt crystal at 520 K, under various gas phase environments.

The photoemission data of cobalt oxides published previously (see Table 1) provide the necessary basis for identification of the cobalt oxidation state [24–30]. In pure O_2, the Co $2p_{3/2}$ photoemission peak at 779.6 eV is accompanied by a weak, broad satellite (marked as S in Fig. 1a) characteristic of the Co_3O_4 spinel phase [24–26]. In agreement, the $L_{3,2}$ edge fine structure (Fig. 1b) is very similar to that previously obtained on Co_3O_4 reference compounds [27,28]. Finally, the Co/O atomic ratio calculated from the Co 2p and O 1s peaks was found 0.69 ± 0.08, within experimental error of the nominal value for Co_3O_4 (0.75). All spectroscopic results are consistent with the complete transformation of cobalt surface to Co_3O_4 when heated in O_2 at 520 K. The thickness of the oxide layer exceeds 4 nm which is the estimated probing depth of the absorption spectra [31]. However, the cobalt crystal is still metallic in the bulk, since photoemission spectra showed no electrostatic charging, as would occur for the electrically insulating bulk Co_3O_4 oxide [26 and reference therein].

The spectroscopic characteristics undergo significant modification in oxygen–methanol mixtures. The Co $2p_{3/2}$ photoemission peak (Fig. 1a) is shifted to higher energies (780.6 eV) and the satellite structure becomes broader and more intense, especially for MR = 2. The difference curve (third spectra from the top), obtained

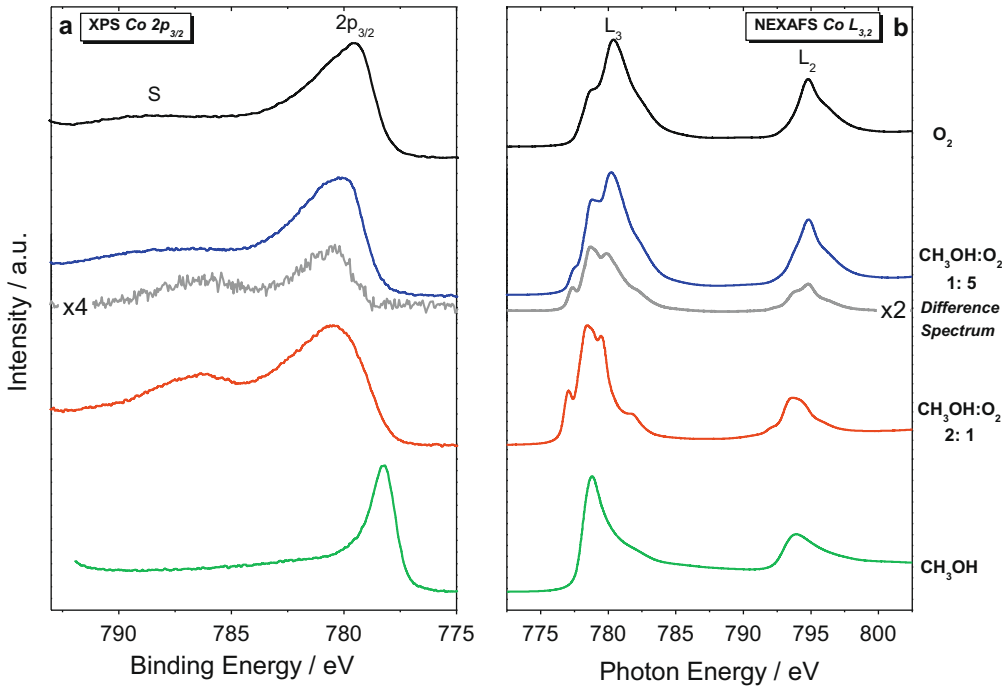

Fig. 1. (a) Co $2p_{3/2}$ XPS ($h\nu$ = 965 eV), and (b) Co $L_{3,2}$ XAS spectra of Co (0 0 0 1) at 520 K under 0.2 mbar O_2, 0.3 mbar $CH_3OH:O_2$ = 1:5, 0.2 mbar $CH_3OH:O_2$ = 2:1 and 0.1 mbar CH_3OH. The difference spectrum between O_2 and $CH_3OH:O_2$ = 1:5 recorded spectra are also showed for comparison.

Table 1
Binding Energy positions of Co $2p_{3/2}$ and O 1s peaks for Co, CoO and Co_3O_4.

	Sample type	Co $2p_{3/2}$ main (eV)	Co $2p_{3/2}$ sat (eV)	O 1s (eV)	Reference
Co_3O_4	Co_3O_4/Co(0 0 0 1)	779.6	788.5 Weak	529.5–530.9	This work
	Powder	779.6 & 780.5	786–789.5 Weak	529.7, 531.3 (Shoulder)	[25]
		779.9			[28]
		779.4		529.2	[29]
		779.8			[31]
		780.0–780.3	789.3		[19] and reference therein
CoO	CoO/Co(0 0 0 1)	780.6	786.3 Strong	529.5–531.2	This work
	CoO/Co(0 0 0 1)	780.1		529.8	[31]
	Powder	780.5	786.2 Strong	529.7, 531.3 (Shoulder)	[25]
	CoO(1 0 0)	780.4	786.7 Strong	529.4	[23]
	Powder	780.3			[29]
		780.4–781.1	787.0, 787.3		[19]
Co	Co	778.3	Weak		This work
	Co(0 0 0 1)	778.3	Weak		[21,31]

after subtraction of Co 2p spectra in pure O_2 and reaction mixture (MR = 0.2), resemble very much that recorded on MR = 2 mixture. These are clear indications for partial reduction of Co_3O_4 under working conditions [24,26]. In pure methanol stream (bottom spectrum), the Co $2p_{3/2}$ peak at 778.3 eV is indicative of cobalt in the metallic state [22,32], verifying that methanol is a very effective reducer for cobalt oxides [7]. The XAS spectra presented in Fig. 1b confirm the photoemission results. In particular, for MR = 0.2 the Co L-edges are the sum of CoO and Co_3O_4 reference spectra, as proved by the difference curve, indicating that under these conditions the surface stoichiometry can be written as CoO_x (with $1 < x < 1.33$). For MR = 2 and pure methanol atmosphere, the Co L-edges are very much alike that found in previous measurements for CoO [27] and metallic cobalt [28], respectively. The strong resemblance of XPS and XAS data on our oxide films grown on Co single crystal, to previous results from CoO and Co_3O_4 bulk oxides is indicative of a similar chemical environment of Co and O ions in the two cases. However, it should be noted that the surface termination of the outermost layers might be considerably different in the two cases, as was recently showed for Co_3O_4 and CoO films grown on iridium [33,34].

It is evident that the composition of the gas phase significantly influences the surface chemical state of cobalt. The key in catalysis is to combine spectroscopic and catalytic data, in other words to correlate the surface chemical state to the catalytic activity and selectivity. Relative selectivities of the main products, as well as the methanol conversion, were calculated based on *on-line* QMS data (Table 2). Depending on the reaction conditions CO, CO_2, CH_2O, H_2O and H_2 were detected. Selectivities refer to constant temperature and pressure conditions (520 K, 0.1–0.3 mbar) and are expressed as the percentage in the overall (CO, CO_2, CH_2O and H_2) production. The maximum activity was obtained just after reaching 520 K (500 K for pure methanol) and afterwards gradual deactivation was observed, as was evident by the decrease of methanol consumption.

Comparison of the spectroscopic and catalytic data presented in Fig. 1 and Table 2 provide direct indications for the catalytic behaviour of cobalt in oxide and metallic form. In particular for MR = 0.2,

Table 2
Relative product selectivities and methanol conversion rates on cobalt, derived by *on-line* QMS results. Data are recorded at 520 K under $CH_3OH:O_2$ reactant gas with mixture ratios 1:5, 2:1 and 1:0.

Methanol-to-oxygen ratio	Maximum methanol conversion (%)	S(CO)	$S(CO_2)$	$S(CH_2O)$	$S(H_2)$	$S(H_2O)$
1:5	26	6	58	13	0	23
2:1	2	25	13	35	16	11
1:0	14	47	0	9	44	0

where Co_3O_4 is the dominant phase, the CH_3OH consumption is high and total oxidation to CO_2 is favoured. In contrast, for MR = 2, partial oxidation products (CO, CH_2O and H_2) are detected, accompanied with significantly lower methanol conversion rates (almost ten times). As showed in Fig. 1, in that case the pre-oxidized cobalt surfaces were reduced to CoO-like oxide. Finally, in a pure CH_3OH stream, metallic cobalt favours methanol decomposition to CO and H_2. It is worth mentioning that above 500 K, a high rate of coke deposition was observed on metallic cobalt, causing fast deactivation of this catalyst.

Combination of in situ spectroscopy and *on-line* gas phase analysis testifies to the dynamic response of the cobalt surface to the reaction mixture, indicating also the effect on the catalytic behaviour. However, for different MRs the reaction kinetics is considerably different, and therefore the assignment of catalytic reactivity exclusively to the cobalt oxidation state is not straightforward. In order to be able to evaluate the intrinsic catalytic properties of cobalt oxides, the comparison must be made under the same reaction mixture and preferably with similar reaction activity.

3.2. The impact of cobalt oxidation state on the catalytic performance

In thermodynamic equilibrium the composition of an oxide surface is determined by the gas phase chemical potential (temperature and oxygen partial pressure) [35]. However, in many cases, significant kinetic barriers inhibit the system from reaching the equilibrium. Therefore, depending on the initial state, various metastable surface compositions can often be maintained under the same chemical potential. In this paragraph we will make use of this principle to compare the intrinsic catalytic properties of cobalt oxides under identical reaction conditions.

As shown in Section 3.1, for MR = 2 the Co_3O_4 is completely reduced to CoO-like oxide, while limited reduction is observed for MR = 0.2. Therefore, in order to compare different cobalt oxidation states under the same reaction conditions, mixtures rich in oxygen (low MRs) should be used. Prior to the reaction, cobalt was treated either in H_2 or in O_2 at 520 K to produce metallic and Co_3O_4 surfaces, respectively. After pre-treatment the samples were cooled at room temperature, where the reaction mixture was introduced, followed by annealing at 520 K. In Fig. 2, spectroscopic and catalytic data recorded on cobalt surfaces pre-treated in H_2 and O_2 are presented. The deconvolution for the different contributions to the overall photoemission and absorption spectra are included in order to facilitate the discussion. In addition the Co:O stoichiometry calculated from O 1s and Co 2p photoemission peaks are presented in Table 3. The reaction conditions (pressure, mixing ratio and temperature) were kept identical and spectra were recorded around 30 min after reaching reaction temperature, where a methanol conversion of 12 ± 3% was measured for both samples. Therefore, relative selectivities presented in Fig. 2c are directly comparable since they refer to similar methanol conversion rates. Both photoemission (Fig. 2a) and absorption (Fig. 2b) spectra of cobalt clearly demonstrate that under the specific reaction conditions, metallic cobalt (pre-treated in H_2) undergoes partial oxidation to CoO-like oxide, whereas the fully oxidized Co_3O_4 surface (pre-treated in O_2) undergoes partial reduction to a 30/70 mixture of CoO/Co_3O_4. This picture is confirmed by the calculated stoichiometry in Table 3.

Depth-dependent measurements of the Co 2p photoemission peaks did not show preferential surface localization of any of the oxides (see F1, Supporting material). Therefore, a layered oxide structure is not supported and it is reasonable to refer either to a mixed CoO_x phase or thick oxide island formation, with x varying according to the pre-treatment. Comparison of spectroscopic results with product selectivities (Fig. 2c) indicates that on the CoO/Co_3O_4 surfaces total combustion to CO_2 is the main reaction path, while on CoO-like surfaces partial oxidation to CH_2O is favoured. Hydrogen formation was not detected and CO production was limited (<5%) in both samples.

The C 1s photoemission spectra recorded under reaction conditions are presented in Fig. 3a. Two carbon components are indicated at binding energies of 286.0 and 288.5 ± 0.1 eV. The peak at 286.0 eV is assigned to surface-adsorbed methoxy groups (CH_3O_{ads}), while the component at 288.5 eV is characteristic of formate species ($HCOO_{ads}$) [5,6,36,37]. The total coverage of carbon species, calculated from their XPS intensities, was found to be the same in the two cases (7.5 ± 0.5%). However, it is evident that the relative amount of methoxy and formate species depends on the pre-treatment, therefore on the oxidation state of the cobalt surface.

The O 1s peak presented in Fig. 3b consists of two oxygen components. The main oxygen component at 529.6 eV is due to lattice oxygen (O_{lat}) of cobalt oxides and its binding energy is not sensitive to the cobalt oxidation state, since both Co_3O_4 and CoO have very similar energies (see Table 1) [25]. The broad oxygen component shift of about 1.9 eV at higher energies cannot be attributed to intrinsic characteristics of cobalt oxides. In addition, depth-depended measurements indicated that this component is mainly located on the surface (see F2, Supporting material). Therefore, the oxygen peak at 531.5 ± 0.1 eV is related to oxygen-containing surface species (O_{surf}) on the cobalt oxide. Unfortunately it is difficult to determine directly the nature of the O_{surf} species. In this energy range various adsorbed species containing oxygen are reported in the literature, like O–H, C–O and C=O species [2,5,6]. The peak at 531.5 eV is definitely a convolution of oxygen related to CH_3O_{ads} and $HCOO_{ads}$ groups, without excluding other types of adsorbed oxygen. In order to test whether adsorbed oxygen species (additionally to formate and methoxy) exist or not, the O_{surf}:C atomic ratio was calculated using photoemission cross sections from reference [23] (the O_{surf} component of the overall O 1s peak derived from the deconvolution procedure shown in Fig. 3b). Assuming that the intensity of O_{surf} is a convolution of three kinds of oxygen species, namely; formate, methoxy and excess oxygen species (O_{exc}), the O_{surf}:C ratio was used to calculate the intensity of O_{exc} on the surface (see Supporting material). It was found that around 30% of the O_{surf} intensity on CoO/Co_3O_4 is due to O_{exc}, while for the CoO – like sample the O_{surf} component is solely due to methoxy and formate species. It should be noted that the nature of O_{exc} cannot be determined accurately due to the overlapping of several oxygen components in the O 1s region.

One of the key observations which arises from the comparison of the spectroscopic and catalytic results in Figs. 2 and 3, is that as the relative amount of CH_3O_{ads} intermediates increases, higher

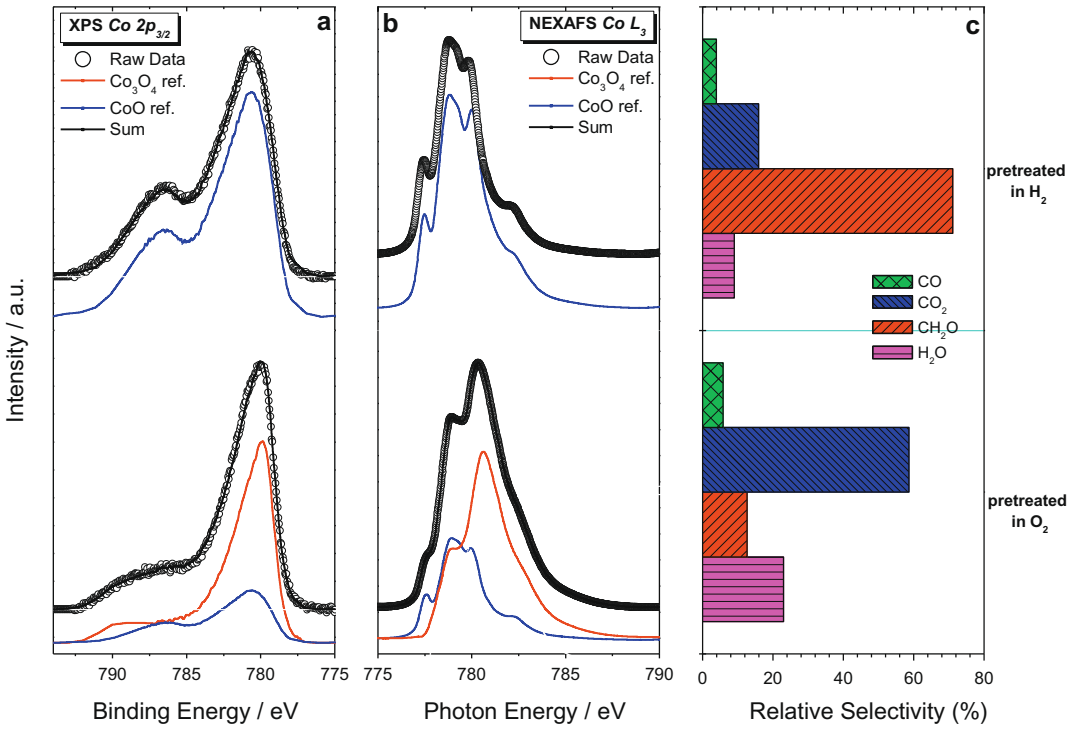

Fig. 2. (a) Co $2p_{3/2}$ XPS ($h\nu$ = 965 eV), (b) Co L_3 NEXAFS spectra, and (c) relative product selectivities, of H_2 and O_2 pre-treated Co(0 0 0 1) samples. Spectroscopic and catalytic data are recorded at 520 K, in CH_3OH:O_2 = 1:5, in total pressure of 0.3 mbar.

Table 3
The Co:O stoichiometry calculated from O 1s and Co 2p photoemission peaks. The reaction conditions were CH_3OH:O_2 = 1:5, total pressure 0.3 mbar and temperature 520 K.

Pretreatment	Stoichiometry Co:O(±0.08)
Hydrogen	0.98
Oxygen	0.73
Co_3O_4	0.69

formaldehyde selectivity is observed. Since the reaction conditions were kept constant, the oxidation state of cobalt apparently has an effect on the relative amount of reaction intermediates and therefore on the selectivity. Fig. 4 summarises the dependence of the CH_2O-to-CO_2 QMS signal ratio (normalized to the maximum ratio), and the cobalt oxide stoichiometry (calculated from the photoemission results), in relation to the relative amount of methoxy species (calculated from the analysis of C 1s photoemission peak). The data are collected on differently pre-treated cobalt surfaces (pure O_2, H_2 and O_2/H_2 mixture) under identical reaction conditions (MR = 0.2 at 520 K). According to this figure, the formaldehyde selectivity (solid cycle points) is positively correlated to the relative abundance of CH_3O_{ads}, and the Co/O atomic ratio (bars). The results presented above indicate that the reaction paths of methanol on cobalt catalysts depend critically on the surface oxidation state.

3.3. Modification of the surface reactivity by chemisorbed species

As has been indicated in Section 3.2, for MR = 0.2, the surface oxidation state influences the adsorbed reaction intermediates. In this paragraph the effect of the gas phase composition on the population and type of adsorbed species will be addressed. In order to avoid complications due to the modification of the surface oxidation state during reaction, a relatively stable substrate must be used to compare different MRs. Obviously, Co_3O_4 is not suitable for such studies since it undergoes fast reduction to CoO in MR = 2, as shown in paragraph 3.1. Therefore CoO pre-formed on the cobalt surface (see Section 2) was used. The surface stoichiometry calculated by the Co 2p and O 1s photoemission peaks, and the conversion-selectivity derived by QMS signal analysis, are presented in Table 4. The initially prepared CoO layer remains practically unaffected in MR = 2, but undergoes partial oxidation in MR = 0.2 (formation of 15% Co_3O_4 at 520 K). This is reflected in the lower Co:O surface stoichiometry (0.89) under 1:5 mixture. The *on-line* QMS results showed that the methanol-to-oxygen mixing ratio affects both the activity and the selectivity of the reaction. In particular, in stationary reaction conditions, the excess of methanol in the mixture increases the selectivity to partial oxidation products (CH_2O, CO, H_2), while in oxygen excess, relatively higher CO_2 production was found. In addition, methanol conversion was almost five times higher for MR = 0.2 compared to MR = 2. It should be noted that, as compared to the cobalt sample with 0.98 Co:O stoichiometry (see Fig. 2), the CO_2 selectivity is favoured here (36 instead of 21%). This is not surprising since as was shown before higher oxygen stoichiometry enhances total oxidation reaction.

Temperature-programmed reaction experiments (TPR) were carried out in order to monitor the evolution of surface intermediate species during the transition from non-reaction to reaction conditions. The surface temperature was increased from 320 to 520 K by 5 K/min. A set of fast photoelectron spectra (Co $2p_{3/2}$, C 1s and O 1s) were recorded approximately every 20 K, (about 50 s each spectrum with variation of temperature during recording around 4 K). In Fig. 5 we compare the development of different types of carbon species (taken from deconvolution of the C 1s peak), with methanol consumption (calculated from *on-line* QMS) for MRs 0.2 and 2. Three carbon components at 285.1, 286.0 and 288.5 ± 0.1 eV were considered for the deconvolution of the overall C 1s peak (see inset of Fig. 5). The C 1s components at 286.0 and 288.5 eV are due to CH_3O_{ads} and $HCOO_{ads}$, respectively, as

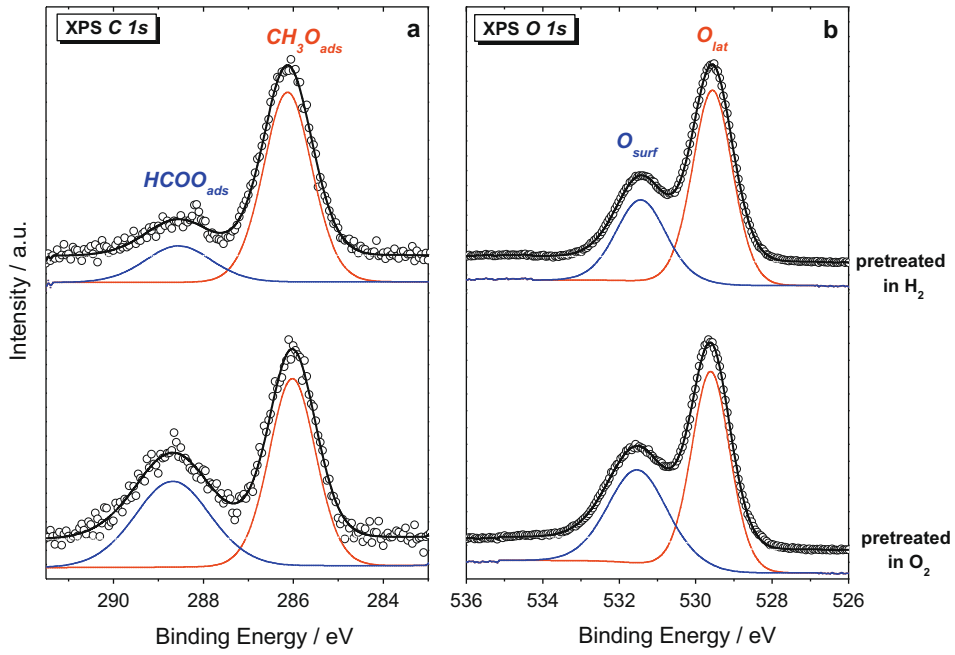

Fig. 3. XPS spectra of: (a) C 1s ($h\nu$ = 475 eV), and (b) O 1s ($h\nu$ = 720 eV) of H_2 and O_2 pre-treated Co(0 0 0 1) sample. Data were recorded at 520 K, in $CH_3OH:O_2$ = 1:5, at total pressure of 0.3 mbar.

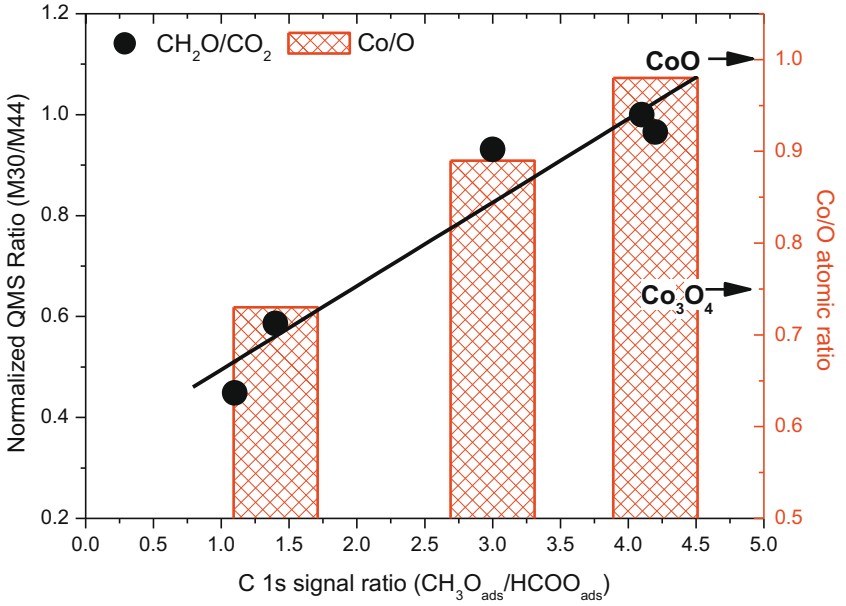

Fig. 4. The CH_2O/CO_2 signal ratio (solid circles) from *on-line* QMS and the cobalt oxide stoichiometry (red bars) as a function of $CH_3O_{ads}/HCOO_{ads}$ ratio (calculated from the analysis of C 1s photoemission peak). The data were collected on differently pre-treated cobalt surfaces (pure O_2, H_2 and O_2/H_2 mixture) under identical reaction conditions ($CH_3OH:O_2$ = 1:5, at 520 K). (For interpretation of the references to colour in this figure legend, the reader is referred to the web version of this article.)

Table 4
The Co:O stoichiometry calculated from photoemission results and normalized product selectivities as well as methanol conversion rate, derived by *on-line* QMS. Data are recorded on a CoO pre-treated substrate at 520 K under $CH_3OH:O_2$ reactant gas with mixture ratios 1:5 and 2:1.

CH_3OH/O_2	Stoichiometry Co:O	Methanol conversion (%)	S(CO)%	$S(CO_2)$%	$S(CH_2O)$%	$S(H_2)$%	$S(H_2O)$%
1:5	0.89	13	8	36	25	0	31
2:1	0.96	2.5	26	10	38	18	8

explained in the previous paragraph. The component at 285.1 eV, which vanishes at high temperatures, is assigned to CH_x species attached to the oxide surface and most probably originates from residual gas phase contaminants in the reaction chamber [5]. The amount of carbon is expressed as the percentage of the maximum carbon coverage (at about 350 K).

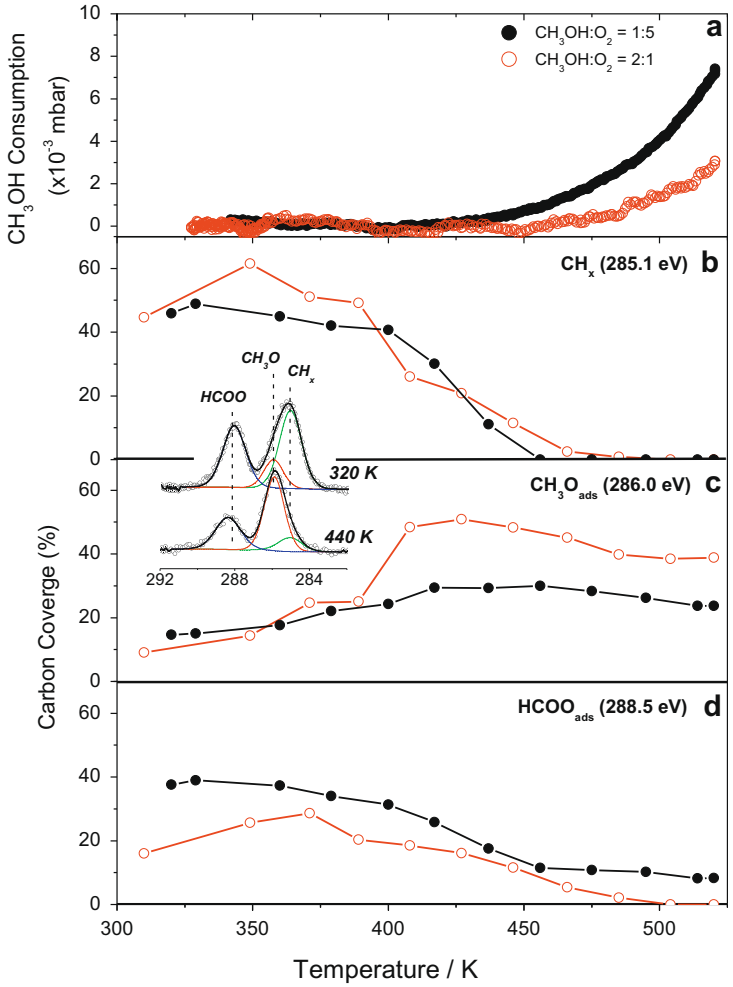

Fig. 5. (a) Methanol consumption, (b) hydrocarbon (c) methoxy, and (d) formate species evolution as a function of temperature for CoO/Co(0 0 0 1) sample, in $CH_3OH:O_2$ = 1:5 (solid cycles) and $CH_3OH:O_2$ = 2:1 (open cycles). The heating rate was 5 K/min.

According to Fig. 5, at low temperatures the surface was mainly covered by hydrocarbon and formate species, which progressively disappearing as the temperature increases. Elimination of these species at 450 K marks the start of catalytic activity as shown in Fig. 5a. In parallel, a significant population of CH_3O_{ads} builds up, which reach a maximum at about 430 K just before ignition of the catalytic activity. Although these general characteristics account for both reaction mixtures there is a substantial difference between the two; in MR = 0.2, a fraction of $HCOO_{ads}$ species remain adsorbed up to 520 K, while in MR = 2 these species are practically removed at about 490 K. In addition, in the lack of $HCOO_{ads}$ (MR = 2), the population of CH_3O_{ads} species is enhanced (see Fig. 5c).

The abundance of CH_3O_{ads} at the expense of $HCOO_{ads}$ species is in qualitative agreement with the increase of partial oxidation products and relatively low CO_2 amounts produced for MR = 2 (see Table 4). However, the higher population of methoxy species for MR = 2 compared with MR = 0.2 (almost 2 times more CH_3O_{ads} species per unit area), is not followed by equally high CH_3OH conversion. On the contrary, the abundance of CH_3O_{ads} at the expense of $HCOO_{ads}$ species is related to the decrease in methanol consumption. Residual carbon impurities or coke formation cannot be blamed for the lower activity in MR = 2 ratio, since only methoxy species are detected on the surface at 520 K. Additionally, apart from oxygen atoms related to formates and methoxy, no additional surface adsorbed oxygen species (O_{exc}) are detected in either mixing ratios, as concluded from the O_{surf}:C ratio analysis. Therefore overpopulation of methoxy species is related to inhibition of the reaction, by poisoning the catalyst surface.

4. Discussion

The present results demonstrate that the active cobalt surface for methanol oxidation reaction is a mixture of CoO and Co_3O_4 like-oxides (CoO_x), with x to depend on the starting compound (metal or oxide) and the composition of the CH_3OH/O_2 reaction mixture. The oxide stoichiometry also determines the reaction path of methanol oxidation over the catalyst. The identification of active cobalt surfaces for partial and total oxidation of methanol to formaldehyde or carbon dioxide respectively, is important for addressing the selectivity issue when new cobalt containing catalysts are designed. Moreover, it is the elementary step towards a better understanding of the methanol reaction mechanism on cobalt and possibly on other oxide surfaces. The mechanism of methanol oxidation discussed in the existing literature, involves different reaction intermediates which lead to diverse products. Formation of methoxy species (CH_3O) is believed to be the first common step for methanol adsorption on both metal and oxide surfaces [19 and reference therein]. In order for methoxy species to further react to CH_2O or CO_2, a proton must be abstracted from a methyl group or an oxygen atom must be attached to it, respectively. The first

process (proton abstraction) requires nucleophile surface sites while the second requires electrophilic oxygen adatoms [2].

The detection of reaction intermediates by in situ XPS depends on their surface coverage, which in turn is determined by their lifetime on the surface. Compared to previous methanol oxidation studies on copper and ruthenium catalysts [4,7], the coverage of formate and methoxy species on cobalt oxide is greatly enhanced (from <2 on Cu to ca. 7% on Co). This indicates that on cobalt, reaction intermediates experience longer lifetimes and are significantly more stable than on copper and ruthenium. As stated above, surface oxygen is crucial for the transformation of methoxy species to CH_2O or CO_2. At low oxygen chemical potential, limited O_2 access on the surface and therefore restriction of adsorbed reactive oxygen species is expected. Consequently the majority of surface sites are occupied by methoxy species and there is only a small fraction of sites containing adsorbed oxygen, leading to suppression of the catalytic activity. In the absence of adsorbed oxygen partial or complete dehydrogenation products (CH_2O, CO, H_2) are expected to be formed according to the reactions:

$$CH_3OH \rightarrow CH_2O + H_2 \quad (1)$$

$$CH_3OH \rightarrow CO + 2H_2 \quad (2)$$

This can explain the experimental results presented in Fig. 5, for MRs = 2 and 0.2 over CoO. In both mixtures, gas phase CH_3OH and O_2 molecules are competing for the same sites on the CoO surface. If adsorbed methanol (CH_3O_{ads}) cannot react with oxygen, it irreversibly blocks the site. This is the case for MR = 2. At high oxygen partial pressure (MR = 0.2) molecular oxygen will be able to compete with methanol for the free sites, whereby the rate of CH_3O_{ads} blocking is limited and higher methanol conversion rates are justified. In the later case the dominant reactions are:

$$CH_3OH + 1/2O_2 \rightarrow CH_2O + H_2O \quad (3)$$

$$CH_3OH + 3/2O_2 \rightarrow CO_2 + 2H_2O \quad (4)$$

Apart from the gas phase oxygen chemical potential, the oxidation state of cobalt is also crucial for the reaction path, as showed in Figs. 2 and 4. Under reaction conditions pure Co_3O_4 phase was not stable and a partially reduced CoO_x ($1 < x < 1.33$) surface oxide was formed. At high x valence of the CoO_x oxide total oxidation is favoured, on lower x, the partial oxidation to CH_2O, and on metallic Co decomposition to CO and H_2. Analogous behaviour was also found for methanol oxidation on ruthenium [7]. High CO_2 production rates are related to equally high formate coverage on the surface (see Fig. 5). Formate species might be formed by addition of one oxygen atom on adsorbed methoxy or formaldehyde species according to the schemes:

$$CH_3O_{ads} + O_{ads} \rightarrow HCOO_{ads} + 2H_{ads} \quad (5)$$

$$CH_2O_{ads} + O_{ads} \rightarrow HCOO_{ads} + H_{ads} \quad (6)$$

Both reactions require participation of electrophilic oxygen species, which involve cobalt ions with reduced electron density. As was previously shown for copper and ruthenium, the incorporation of sub-surface oxygen into the first surface layers modifies the local electronic structure of metal ions and favours the formation of electrophilic oxygen. In addition it might cause surface lattice strain which relaxes by surface roughening and thus generates new active sites [2]. On cobalt the lattice strain and the local electronic structure near the surface tailor to the cobalt oxidation state, as was recently demonstrated by combined STM and LEED studies [33,34]. Theoretical studies on the Co_3O_4(1 1 0) surface also predicted oxygen adsorption sites with different electron affinities [38]. It is however difficult to distinguish those sites on a cobalt oxide surface, as was previously done for copper [4], due to the complexity of the O 1s photoemission peak.

The similarities of methanol oxidation on cobalt, to previous studies on copper and ruthenium are quite profound. On copper the electron density of surface atoms is modified by sub-surface oxygen species [4], while for ruthenium, a "transient surface oxide (RuO_x)" formed under specific reaction conditions, was found to be catalytically active [6]. On cobalt, oxidation is extended to several layers (>4 nm), so it is reasonable to refer to a thick surface oxide layer, at least under the reaction conditions examined here. The stoichiometric Co_3O_4 oxide was only observed in pure oxygen atmosphere, while in the presence of methanol a mixture of CoO/Co_3O_4 was always present (CoO_x). This is in good agreement with the observations on ruthenium where a transient ruthenium oxide and not RuO_2 was the active phase for methanol oxidation [6,7]. A simple comparison of the geometric structures of spinel (Co_3O_4) and rocksalt (CoO) oxides can provide additional insights into the reaction mechanism. The lattice oxygen of both oxides is face centred cubic (fcc) type [25,26]. Oxygen ions on the Co_3O_4 surface are highly mobile, compared to CoO, as supported by the ease of reducibility of cobalt oxides which has been shown to be in the order of $Co_3O_4 > CoO$ [17]. It is reasonable to assume that the higher mobility of oxygen species in Co_3O_4 will assist their migration on the outermost surface layer when thermodynamic conditions are favourable. In the reduction step, Co_3O_4 can be an effective electron acceptor i.e. $Co^{3+} + e^- \rightarrow Co^{2+}$, with oxygen ions providing the electronic charge for Co^{3+} reduction. According to the reactivity pattern discussed before for Cu and Ru, when oxygen ions have less electronic charge, they become more electrophilic favouring methanol combustion. In high oxygen chemical potential (MR = 0.2) reoxidation of Co^{2+} sites by gas phase oxygen will create a CoO/Co_3O_4 mixture on the surface, as shown in Fig. 2. The stability of the catalyst is determined by the capability of oxygen to incorporate into the cobalt surface, i.e. the ability to reoxidize the reduced sites with gas phase oxygen. The chemical potential of gas phase oxygen is a key factor in this process as shown here. In low oxygen chemical potentials complete reduction of Co_3O_4 to CoO will favour building of nucleophilic oxygen and therefore selective reaction paths.

5. Conclusions

Combination of in situ photoelectron and absorption spectroscopies with *on-line* mass spectrometry was employed to investigate methanol oxidation on cobalt in the mbar pressure range. The results showed that methanol is capable of reacting with both oxidized and metallic cobalt surfaces. The reaction path strongly depends on the cobalt oxidation state and the methanol-to-oxygen mixing ratio (oxygen chemical potential). The stoichiometric Co_3O_4 phase is stable only in oxygen atmosphere and is partially reduced under reaction conditions to a mixed Co_3O_4/CoO oxide. Depending on the prevailing oxide phase the preferential reaction channels are: (a) for Co_3O_4, total oxidation to CO_2 and H_2O, and (b) for CoO, the partial oxidation to CH_2O. Metallic cobalt is readily oxidized to CoO even in methanol rich environments, while in the absence of oxygen in the gas phase it favours methanol decomposition to CO and H_2. The chemical potential of gas phase oxygen not only determines the surface oxidation state, but also the relative population of reaction intermediates (CH_3O_{ads} and $HCOO_{ads}$). It can be argued that the formaldehyde formation is not only determined by the abundance of CH_3O_{ads} species, but also by the availability of surface oxygen ions. Finally, comparison with previous studies on ruthenium and copper indicated that the transient surface oxide phase proposed earlier, might also account for the reactivity pattern on cobalt surfaces.

Acknowledgements

S.Z. and T.D. gratefully acknowledge the BESSY II EUSA programme for financial support during the experiments conducted at BESSY II. The authors would like to thank the BESSY II staff for their help in carrying out the experiments.

Appendix A. Supplementary material

Supplementary data associated with this article can be found, in the online version, at doi:10.1016/j.jcat.2009.11.013.

References

[1] H. Topsøe, J. Catal. 216 (2003) 155.
[2] M. Salmeron, R. Schlögl, Surf. Sci. Rep. 63 (2008) 169.
[3] G. Rupprechter, C. Weilach, Nanotoday 2 (2007) 20.
[4] H. Bluhm, M. Hävecker, A. Knop-Gericke, E. Kleimenov, R. Schlögl, D. Teschner, V.I. Bukhtiyarov, D.F. Ogletree, M. Salmeron, J. Phys. Chem. B 108 (2004) 14340.
[5] S. Günther, L. Zhou, M. Hävecker, A. Knop-Gericke, E. Kleimenov, R. Schlögl, R. Imbihl, J. Chem. Phys. 125 (2006) 114709.
[6] R. Blume, M. Hävecker, S. Zafeiratos, D. Teschner, E. Vass, P. Schnorch, A. Knop-Gericke, R. Schlögl, S. Lizzit, P. Dudin, A. Barinov, M. Kiskinova, Phys. Chem. Chem. Phys. 9 (2007) 3648.
[7] R. Blume, M. Hävecker, S. Zafeiratos, D. Teschner, A. Knop-Gericke, R. Schlögl, P. Dudin, A. Barinov, M. Kiskinova, Catal. Today 124 (2007) 71.
[8] J. Zhang, J. Chen, J. Ren, Y. Sun, Appl. Catal. A 243 (2003) 121.
[9] M. Voß, D. Borgmann, G. Wedler, J. Catal. 212 (2002) 10.
[10] E. Iglesia, Appl. Catal. A 161 (1997) 59.
[11] G.P. Van der Laan, A.A.C.M. Beenackers, Catal. Rev. Sci. Eng. 41 (1999) 255.
[12] B. Kerler, A. Martin, A. Jans, M. Baerns, Appl. Catal. A 220 (2001) 243.
[13] Y. Zhang, K.J. Smith, Catal. Today 77 (2002) 257.
[14] L.B. Avdeeva, D.I. Kochubey, Sh.K. Shaikhutdinov, Appl. Catal. A 177 (1999) 43.
[15] J. Llorca, P.R. de la Piscina, J.-A. Dalmon, J. Sales, N. Homs, Appl. Catal. B 43 (2003) 355.
[16] M. Ni, D.Y.C. Leung, M.K.H. Leung, Int. J. Hydrogen Energy 32 (2007) 3238.
[17] S. Tuti, F. Pepe, Catal. Lett. 122 (2008) 196.
[18] J. Jansson, A.E.C. Palmqvist, E. Fridell, M. Skoglundh, L. Osterlund, P. Thormahlen, V. Lange, J. Catal. 211 (2002) 387.
[19] M.M. Natile, A. Glisenti, Chem. Mater. 14 (2002) 3090.
[20] K. Habermehl-Cwirzen, J. Lahtinen, P. Hautojärvi, Surf. Sci. 598 (2005) 128.
[21] O. Skoplyak, C.A. Menning, M.A. Barteau, J.G. Chen, J. Chem. Phys. 127 (2007) 114707.
[22] M.P. Seah, in: D. Briggs, M.P. Seah (Eds.), Practical Surface Analysis, second ed., Willey & Sons, Chichester, UK, 1992. vol. 1.
[23] J.J. Yeh, I. Lindau, At. Data Nucl. Data Tables 32 (1985) 1.
[24] S.C. Petitto, E.M. Marsh, G.A. Carson, M.A. Langell, J. Mol. Catal. A: Chem. 281 (2008) 49.
[25] M.A. Langell, J.G. Kim, D.L. Pugmire, W. McCarroll, J. Vac. Sci. Technol. A 19 (2001) 1977.
[26] H.A.E. Hagelin-Weaver, G.B. Hoflund, D.M. Minahan, G.N. Salaita, Appl. Surf. Sci. 235 (2004) 420.
[27] D. Bazin, I. Kovács, L. Guczi, P. Parent, C. Laffon, F. De Groot, O. Ducreux, J. Lynch, J. Catal. 189 (2000) 456.
[28] T.J. Regan, H. Ohldag, C. Stamm, F. Nolting, J. Lüning, J. Stöhr, R.L. White, Phys. Rev. B 64 (2001) 214422.
[29] W.-H. Yang, M.H. Kim, S.-W. Ham, Catal. Today 123 (2007) 94.
[30] J. van Elp, J.L. Wieland, H. Eskes, P. Kuiper, G. Sawatzky, Phys. Rev. B 44 (1991) 6090.
[31] M. Abbate, J.B. Goedkoop, F.M.F. de Groot, M. Grioni, J.C. Fuggle, S. Hofmann, H. Petersen, M. Sacchi, Surf. Interf. Anal. 18 (1992) 65.
[32] I. Nakamura, M. Haneda, H. Hamada, T. Fujitani, J. Electron Spectrosc. Relat. Phenom. 150 (2006) 150.
[33] W. Meyer, D. Hock, K. Biedermann, M. Gubo, S. Mueller, L. Hammer, K. Heinz, Phys. Rev. Lett. 101 (2008) 016103.
[34] W. Meyer, K. Biedermann, M. Gubo, L. Hammer, K. Heinz, J. Phys.: Condens. Matter. 20 (2008) 265011.
[35] M. Batzill, U. Diebold, Prog. Surf. Sci. 79 (2005) 47.
[36] M. Shen, F. Zaera, J. Phys. Chem. C 112 (2008) 1636.
[37] T. Kawabe, K. Tabata, E. Suzuki, Y. Nagasawa, Surf. Sci. 482–485 (2001) 183.
[38] P. Broqvist, I. Panas, H. Persson, J. Catal. 210 (2002) 198.